Supporting information

Table S1. *Three molecular dynamics simulations carried out in this study.*

Simulation name	**Production run duration (ns)**	**Box dimension (Å)**	**Total number of atoms**	**Number of lipids (POPC/POPE/ cholesterol)**	**Number of water molecules**
Simulation 1	700	90x90x180	147359	240 (96/96/48)	29342
Simulation 2	700	90x90x180	147359	240 (96/96/48)	29342
Simulation 3	1200	90x90x180	147359	240 (96/96/48)	29342

***Table S2**. Comparison of characteristic distances of the conformational state in pentameric ligand-gated ion channels experimental structures.*

System	State[a]	Identifier[b]	C-loop opening (Å)[c]	Activation distance (Å)[d]	Pore radius (Å)	
					Position 9'[e]	Position 16'[f]
α4β2 nAChR	Resting	This study	13.2 ± 1.0[g]	6.3 ± 0.7[g]	1.6	1.4
	Desensitized	5kxi[h]	8.2 ± 0.2	3.7 ± 0.0	4.5	5.0
GlyR1	Open	3jae[i]	11.0 ± 0.0	4.4 ± 0.0	7.2	7.2
	Resting	3jad[i]	14.3 ± 0.0	7.8 ± 0.0	1.3	3.6
	Desensitized	3jaf[i]	11.1 ± 0.0	4.2 ± 0.0	7.4	4.3
GlyR3	Resting	5cfb[j]	13.6 ± 0.2	8.3 ± 0.1	1.3	3.5
	Desensitized	5tio[k]	9.1 ± 0.1	4.4 ± 0.0	4.9	8.1
GLIC	Open	4zzc[l]	8.7 ± 0.2	4.4 ± 0.0	3.1	5.5
	Resting	4lmj[m]	9.4 ± 0.2	6.8 ± 0.1	1.8	2.2
GluCl	Resting	4tnv[n]	11.2 ± 0.3	6.7 ± 0.0	1.3	3.8
	Desensitized	3ri5[o]	10.6 ± 0.1	4.6 ± 0.0	3.1	7.0
GABAAR	Desensitized	4cof[p]	10.4 ± 0.1	4.5 ± 0.0	5.6	9.2
5-HT3	Resting	4pir[q]	19.8 ± 0.5	6.3 ± 0.1	2.3	3.3
ELIC	Resting	2vl0[r]	12.0 ± 0.2	6.3 ± 0.0	1.6	1.0

[a] The activation state as suggested by the authors of the corresponding structures.

[b] The Protein Data Bank identifier of each structure and literature reference.

[c] The opening of the C-loop is defined as the distance between a Cα atom in the C-loop and a Cα atom in a β-strand of the complementary subunit. The residues used to define this distance are: α4 C199–S38 for 5kxi; N219–F79 for 3jad, 3jae and 3jaf; N203–F44 for 5cfb and 5tio; E177–Y23 for 4zzc; E176–Y22 for 4lmj; N196–L35 for 4tnv and 3ri5; A201–D43 for 4cof; I203–I44 for 4pir; and L178–F19 for 2vl0.

[d] The linker distance is defined as the distance between a Cα atom of the β1-β2 inker (the left residue in the bracket) and a Cα atom of the M2-M3 linker (the right residue in the bracket). This activation distance is defined as the distance between: α4 K53–P271 and β2 R48–P263 for 5kxi; T70–P291 for 3jad, 3jae and 3jaf; T54–P275 for 5cfb and 5tio; C33–P247 for 4zzc; C33–P247 for 4lmj; V45–P268 for 4tnv and 3ri5; V53–P273 for 4cof; K54–P274 for 4pir; and L29–P254 for 2vl0.

[e] Residues corresponding to 9' are: α4 L257 and β2 L249 for 5kxi; L277 for 3jad, 3jae and 3jaf; L261 for 5cfb and 5tio; I233 for 4zzc; I232 for 4lmj; L254 for 4tnv and 3ti5; L259 for 4cof; L260 for 4pir; and L239 for 2vl0.

[f] Residues corresponding to 16' are: α4 L264 and β2 L256 for 5kxi; S284 for 3jad, 3jae and 3jaf; S268 for 5cfb and 5tio; I240 for 4zzc; I239 for 4lmj; A261 for 4tnv; and 3ri5, T266 for 4cof, I268 for 4pir, and F246 for 2vl0.

[g] This values is ± standard deviation computed after 400 ns MD simulation for the three simulations; all other values in the table are ± standard deviation computed on all equivalent subunits in the final frame of the MD simulation or in the experimental structures.

[h] Morales-Perez CL, Noviello CM, Hibbs RE (2016) X-ray structure of the human α4β2 nicotinic receptor. *Nature* 538(7625):411–415.

[i] Du J, Lü W, Wu S, Cheng Y, Gouaux E (2015) Glycine receptor mechanism elucidated by electron cryo-microscopy. *Nature* 526(7572):277–280.

[j] Huang X, Chen H, Michelsen K, Schneider S, Shaffer PL (2015) Crystal structure of human glycine receptor-α3 bound to antagonist strychnine. *Nature* 526(7572):277–80.

[k] Huang X, et al. (2017) Crystal structures of human glycine receptor α3 bound to a novel class of analgesic potentiators. *Nat Struct Mol Biol* 24(2):108–113.

[l] Sauguet L, Fourati Z, Prangé T, Delarue M, Colloc'h N (2016) Structural Basis for Xenon Inhibition in a Cationic Pentameric Ligand-Gated Ion Channel. *PloS One* 11(2):e0149795.

[m] Gonzalez-Gutierrez G, Cuello LG, Nair SK, Grosman C (2013) Gating of the proton-gated ion channel from Gloeobacter violaceus at pH 4 as revealed by X-ray crystallography. *Proc Natl Acad Sci U S A* 110(46):18716–18721.

[n] Althoff T, Hibbs RE, Banerjee S, Gouaux E (2014) X-ray structures of GluCl in apo states reveal a gating mechanism of Cys-loop receptors. *Nature* 512(7514):333–337.

[o] Hibbs RE, Gouaux E (2011) Principles of activation and permeation in an anion-selective Cys-loop receptor. *Nature* 474(7349):54–60.

[p] Miller PS, Aricescu AR (2014) Crystal structure of a human GABAA receptor. *Nature* 512(7514):270–275.

[q] Hassaine G, et al. (2014) X-ray structure of the mouse serotonin 5-HT_3 receptor. *Nature* 512(7514):276–281.

[r] Hilf RJC, Dutzler R (2008) X-ray structure of a prokaryotic pentameric ligand-gated ion channel. *Nature* 452(7185):375–379.

Table S3. *Distance characteristic of the C-loop opening in crystal structures of AChBP in complex with agonists and antagonists ligands.*

Identifier[a]	AChBP strain[b]	C-loop opening distance (Å)[c]	Activity[d]	Ligand
2xz5	*A. californica*	9.8	Agonist	Acetylcholine
2byq	*A. californica*	10.0	Agonist	Epibatidine
1uv6	*L. stagnalis*	10.1	Agonist	Carbamylcholine
1uw6	*L. stagnalis*	10.1	Agonist	Nicotine
2wnc	*A. californica*	10.3	Agonist	Tropisetron
2zjv	*L. stagnalis*	10.6	Agonist	Clothianidin
4bqt	*A. californica*	10.6	Agonist	Cytisine
2wnl	*A. californica*	10.7	Agonist	Anabaseine
3c84	*A. californica*	10.7	Agonist	Thiacloprid
2bys	*A. californica*	10.4	Agonist/antagonist	Lobeline
4afh	*C. teleta*	12.7	Agonist/antagonist	Lobeline
3c79	*A. californica*	11.5	Agonist/antagonist	Imidacloprid
2zju	*L. stagnalis*	12.9	Agonist/antagonist	Imidacloprid
4alx	*L. stagnalis*	12.7	Antagonist	DhβE
2x00	*A. californica*	13.2	Antagonist	Gymnodimine A
2xyt	*A. californica*	14.6	Antagonist	*d*-Tubocurarine
3peo	*A. californica*	14.6	Antagonist	Metocurine
2byr	*A. californica*	15.0	Antagonist	Methyllycaconitine
2wzy	*A. californica*	15.0	Antagonist	13-desmethyl spirolide C
2pgz	*A. californica*	15.8	Antagonist	Cocaine
4ez1	*A. californica*	17.6	Antagonist	α-Conotoxin BuIA
2br8	*A. californica*	18.0	Antagonist	α-Conotoxin PnIA variant
5jme	*A. californica*	18.3	Antagonist	α-Conotoxin PeIA
5co5	*A. californica*	18.4	Antagonist	α-Conotoxin GIC
2c9t	*A. californica*	18.6	Antagonist	α-Conotoxin ImI
2uz6	*A. californica*	18.6	Antagonist	α-Conotoxin TxIA variant
1yi5	*L. stagnalis*	20.0	Antagonist	α-cobratoxin
5t90	*L. stagnalis*	20.3	Antagonist	α-Conotoxin LsIA

[a] The Protein Data Bank identifier of each structure.

[b] Organism from which the AChBP was originally extracted: *Lymneae stagnalis*, *Aplysia californica* or *Capitella teleta*

[c] Distance characteristic of the C-loop opening, which is taken between the Cα of C187 and K34 for *Lymneae stagnalis* AChBP and between the Cα of C183 and T34 for *Aplysia californica* AChBP.

[d] Type of Activity of the ligand on nAChR receptors. Some ligands can be agonists or antagonists depending

of the nAChR subtype.

Table S4. Experimental structures and tilt angles represented in Figure 6C.

Receptor	State	Identifier[a]	ECD radial tilt angle (°)[b]	M2 radial tilt angle (°)[c]
nAChR	Resting	This study	4.61	2.87
nAChR	Desensitized	5kxi	0.39	8.45
5-HT_3	Resting	4pir	0.97	5.01
5-HT_3	Resting	6be1	1.60	4.01
ELIC	Resting	2vl0	0.13	3.74
ELIC		2yks	0.30	4.48
ELIC		2yn6	0.14	3.04
ELIC		2yoe	0.18	3.26
ELIC		3rqu	0.53	3.03
ELIC		3rqw	0.94	3.01
ELIC		3uq4	0.47	4.64
ELIC		3uq5	0.58	4.83
ELIC		3uq7	0.51	4.72
ELIC		3zkr	0.42	3.30
ELIC		4a97	0.17	3.54
ELIC		4a98	0.29	3.06
ELIC		4twd	0.58	4.92
ELIC		4twf	0.41	4.12
ELIC		4twh	0.58	4.52
ELIC		4z90	0.33	3.20
ELIC		4z91	0.26	2.90
ELIC		5hej	1.46	2.95
ELIC		5heo	0.94	3.43
ELIC		5heu	1.02	2.68
ELIC		5hew	1.41	3.35
ELIC		5lg3	1.14	3.26
ELIC		5lid	1.23	3.10
ELIC		5sxu	0.37	2.58
ELIC		5sxv	0.29	2.55
$GABA_AR$	Desensitized	4cof	1.07	9.86
GLIC	Resting	4lmj	8.57	3.70
GLIC	Desensitized	5j0z	7.41	7.18
GLIC	Open	4zzc	7.69	6.59
GLIC	Open	5v6n	7.04	6.90
GLIC		2xq3	7.59	7.26
GLIC		2xq4	7.63	6.98
GLIC		2xq5	7.49	7.19
GLIC		2xq6	7.52	7.61

GLIC	2xq7	7.90	7.87
GLIC	2xq8	7.52	8.52
GLIC	2xqa	7.63	6.93
GLIC	3eam	7.82	6.66
GLIC	3ehz	7.15	7.25
GLIC	3lsv	7.73	6.69
GLIC	3p4w	7.28	6.98
GLIC	3p50	7.31	6.91
GLIC	3tlt	8.00	3.30
GLIC	3tlu	7.64	3.17
GLIC	3tlv	7.82	2.12
GLIC	3uu8	7.85	6.58
GLIC	4f8h	7.78	6.96
GLIC	4hfb	7.88	6.66
GLIC	4hfc	7.43	6.89
GLIC	4hfd	7.54	6.93
GLIC	4hfe	7.80	6.86
GLIC	4hfh	7.55	7.01
GLIC	4hfi	7.80	6.91
GLIC	4il4	7.72	7.10
GLIC	4il9	7.40	6.73
GLIC	4ila	7.85	6.80
GLIC	4ilb	7.50	7.36
GLIC	4ilc	7.51	6.94
GLIC	4ire	7.47	7.30
GLIC	4qh5	7.78	7.01
GLIC	4zzb	7.70	2.30
GLIC	5heg	7.74	4.00
GLIC	5heh	7.23	7.24
GLIC	5iux	8.34	7.02
GLIC	5mur	7.37	6.67
GLIC	5mvn	7.28	7.35
GLIC	5mzq	7.29	7.22
GLIC	5mzr	7.35	7.55
GLIC	5mzt	7.31	7.49
GLIC	5v6o	7.12	6.62
GLIC	6f0i	8.00	6.39
GLIC	6f0j	7.83	6.47
GLIC	6f0m	8.05	6.54
GLIC	6f0n	8.02	6.50
GLIC	6f0r	7.25	7.11

GLIC		6f0u	7.94	6.48
GLIC		6f0v	7.44	7.08
GLIC		6f0z	7.53	7.04
GLIC		6f10	8.25	7.07
GLIC		6f11	7.64	6.97
GLIC		6f12	8.32	7.04
GLIC		6f13	7.53	6.95
GLIC		6f15	7.50	6.99
GLIC		6f16	7.51	7.14
GLIC		6f7a	10.07	2.76
GluCl	Resting	4tnv	11.25	0.90
GluCl	Desensitized	3ri5	6.08	5.88
GluCl		3rhw	6.18	5.80
GluCl		3ria	5.86	5.53
GluCl		3rif	5.80	5.88
GlyR1	Resting	3jad	4.95	2.81
GlyR1	Desensitized	3jaf	1.51	6.44
GlyR1	Open	3jae	0.92	2.55
GlyR3	Resting	5cfb	5.55	4.91
GlyR3	Desensitized	5tio	1.46	9.20
GlyR3		5tin	1.39	8.94
GlyR3		5vdh	1.31	8.02
GlyR3		5vdi	1.25	7.87

[a] The Protein Data Bank identifier of each structure.

[b] The extracellular domain (ECD) tilt angle averaged over the five subunits of each structure. This angle is defined in Figure 4.

[c] The transmembrane helix 2 (M2) tilt angle averaged over the five subunits of each structure. This angle is defined in Figure 6.

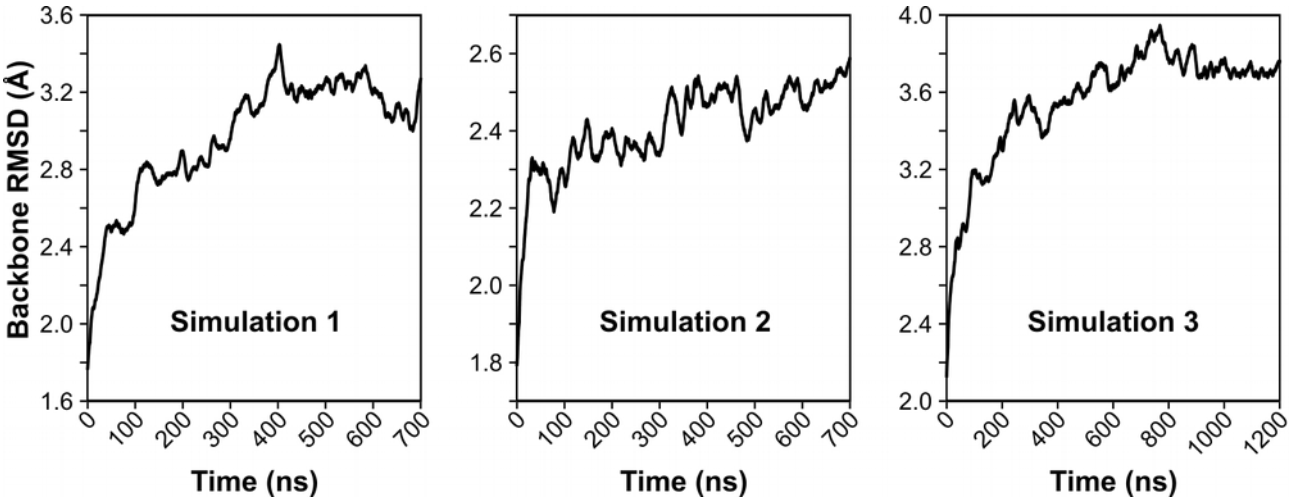

Figure S1. Backbone root-mean-square deviation from the initial conformation measured during the production run of the three molecular dynamocs simulations.

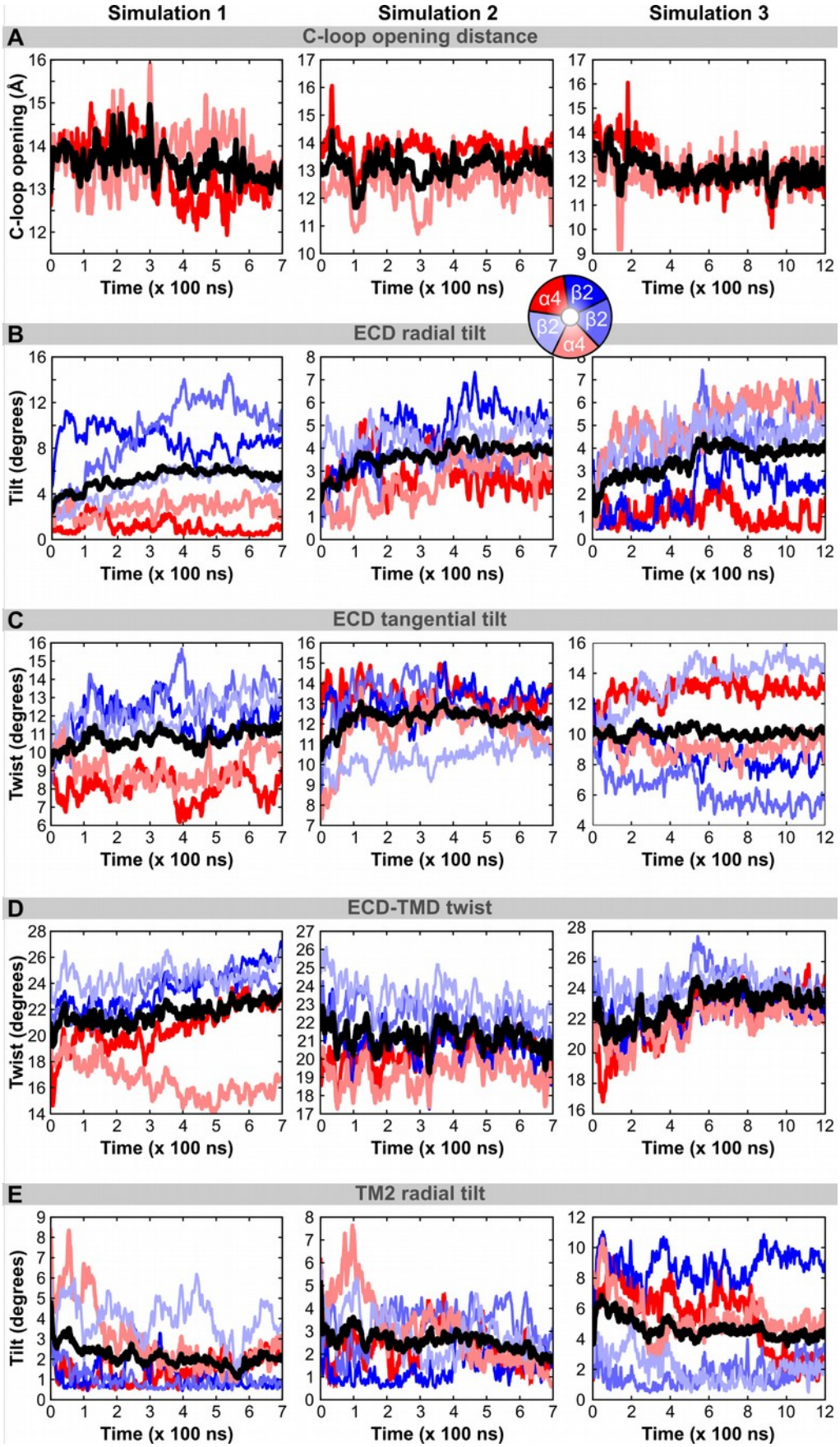

Figure S2. Analysis of the change of conformation of each subunit of the α4β2 nAChR during the three MD simulations. *(A) Change of conformation of the C-loop (defined in Figure 3). (B, C)*

Evolution of the radial and tangential tilt (defined in Figure 4). (D) Evolution of the ECD-TMD twist angle (defined in Figure 4). (E) Evolution of M2 radial tilt angle (defined in Figure 6). The graphics on the left, middle and right are for Simulations 1, 2 and 3, respectively. The red and blue lines represent different subunits as defined in the circular key that represents the arrangement of α4 and β2 subunits in the receptor.

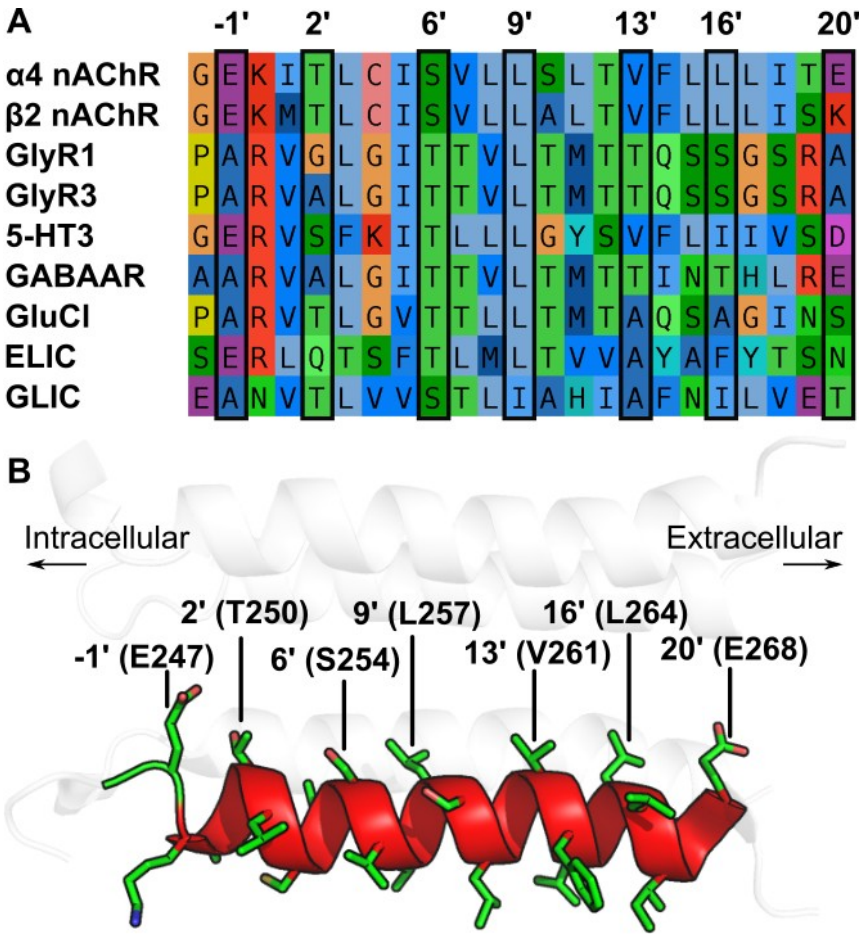

Figure S3. M2 sequence and structure with identification of positions lining the pore. *(A) Amino acids sequence alignment of the M2 helix of several Cys-loop receptors. The positions lining the pores are boxed. (B) Structure of the M2 helix of the α4 nAChR subunit with residues lining the pore labelled. The other M2 helices forming the transmembrane pore of the α4β2 nAChR are represented in transparency. The positions are numbered using the M2 standard numbering from -1' to 20' and the absolute numbering of the positions are indicted between parentheses.*

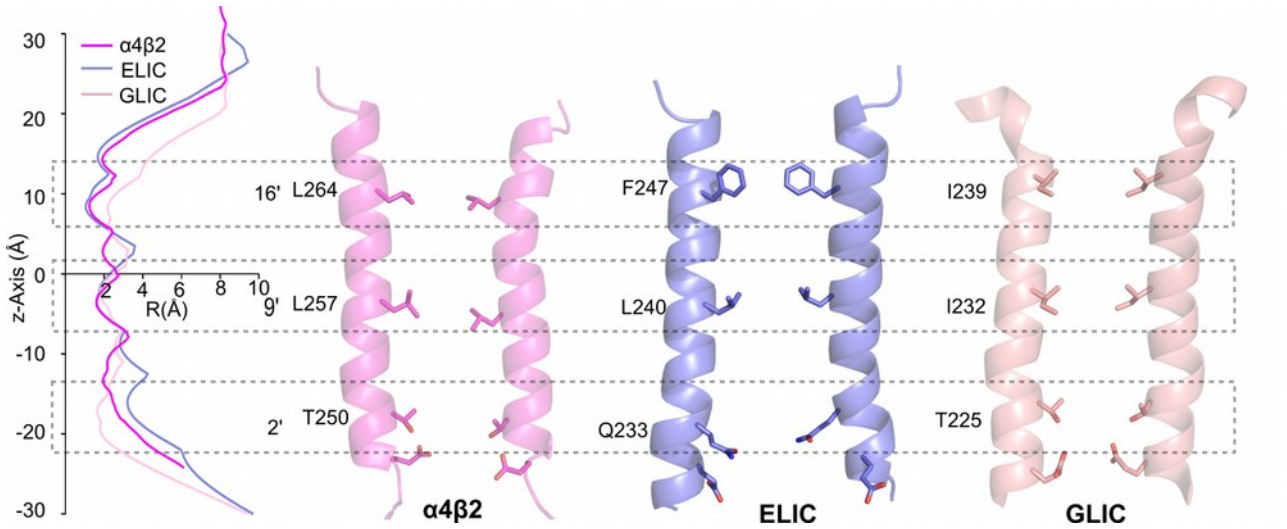

***Figure S4*. Comparison of the M2 of α4β2 nAChR with the corresponding domain of ELIC and GLIC in closed/resting state.** *The M2 helix of α4β2 nAChR (magenta) is from the last frame in 700ns MD simulation of the α4β2 nAChR bound with DHβE; M2 of ELIC and GLIC are corresponding to the M2 of the crystal structure of ELIC (PDB identifier 5gl3) and crystal structure of GLIC (PDB identifier 4lmj), respectively. Orientation of the M2 helix between α4β2 nAChR, ELIC and GLIC is very similar nearly parallel to the z-axis. The hydrophobic residues at 9' and 16' positions constitute the hydrophobic gate or girdle of the M2 domain of the α4β2 nAChR, ELIC and GLIC in closed/resting state.*